Structure-Function Analysis of Tritrpticin Analogs: Potential Relationships between Antimicrobial Activities, Model Membrane Interactions, and Their Micelle-Bound NMR Structures

David J. Schibli,* Leonard T. Nguyen,* Stephanie D. Kernaghan,* Øystein Rekdal,† and Hans J. Vogel*
*Structural Biology Research Group, Department of Biological Sciences, University of Calgary, Calgary, Alberta, Canada; and †Institute of Medical Biology, Faculty of Medicine, University of Tromsø, Tromsø, Norway

ABSTRACT Tritrpticin is a member of the cathelicidin family of antimicrobial peptides. Starting from its native sequence (VRRFPWWWPFLRR), eight synthetic peptide analogs were studied to investigate the roles of specific residues in its biological and structural properties. This included amidation of the C-terminus paired with substitutions of its cationic and Phe residues, as well as the Pro residues that are important for its two-turn micelle-bound structure. These analogs were determined to have a significant antimicrobial potency. In contrast, two other peptide analogs, those with the three Trp residues substituted with either Phe or Tyr residues are not highly membrane perturbing, as determined by leakage and flip-flop assays using fluorescence spectroscopy. Nevertheless the Phe analog has a high activity; this suggests an intracellular mechanism for antimicrobial activity that may be part of the overall mechanism of action of native tritrpticin as a complement to membrane perturbation. NMR experiments of these two Trp-substituted peptides showed the presence of multiple conformers. The structures of the six remaining Trp-containing analogs bound to dodecylphosphocholine micelles showed major, well-defined conformations. These peptides are membrane disruptive and show a wide range in hemolytic activity. Their micelle-bound structures either retain the typical turn-turn structure of native tritrpticin or have an extended α-helix. This work demonstrates that closely related antimicrobial peptides can often have remarkably altered properties with complex influences on their biological activities.

INTRODUCTION

In recent years, there has been an increasing interest in understanding the antimicrobial mechanism of the tryptophan-rich (Trp-rich) class of antimicrobial peptides (1). The best studied of the Trp-rich class of peptides is indolicidin (2) for which there have been numerous structure-function studies performed (3–8). The primary sequence of tritrpticin is very similar to that of indolicidin; both have five aromatic residues, and multiple Pro and basic residues (9). Tritrpticin has an extra positive charge compared to indolicidin with the four positively charged residues of tritrpticin equally localized to the N- and C-termini.

After the initial description of tritrpticin and the NMR structure determination in sodium dodecyl sulfate micelles (SDS) (9,10), several structure-function analyses of tritrpticin have been performed to better understand the mechanism of action of the peptide and improve its efficacy as an antimicrobial agent (11–13). For example, because the sequence of tritrpticin is very nearly palindromic, Nagpal et al. (11) designed a variant of tritrpticin in which Val-1 and Leu-11 were removed to create a symmetric peptide, which was significantly more active than the parent molecule. In fact, Val-1 is probably not present nor essential in the native peptide, because this residue is likely removed during the proteolytic cleavage of the parent cathelicidin pro-domain (14). Indeed, removal of the terminal Val does not significantly alter the activity of the peptide (11). This is also in agreement with the fact that there are no observable interactions between Val-1 and the rest of the micelle-bound peptide (10).

In this work, we have studied several analogs of tritrpticin in which changes were introduced to perturb its membrane binding properties and/or its membrane-bound structure. A first change that we introduced is the amidation of the carboxy-terminal end of the tritrpticin. This substitution is found naturally in indolicidin and removes the sole negative charge of these peptides. This substitution is expected to give rise to a higher antimicrobial activity because it would reduce the electrostatic repulsion between the C-terminus of the peptides and the phosphodiester group of the phospholipids. A second change involves altering the aromatic residues. As is commonly observed for antimicrobial peptides (15), replacement of the three Trp residues of tritrpticin by Ala abolishes the antimicrobial activity (12). We therefore elected to replace the three Trp residues with Phe or Tyr. Replacement of Trp with Tyr is seemingly attractive because its side chain, like that of Trp, prefers to locate itself in the membrane interface, whereas the side chain of Phe typically penetrates deeper into the central portion of the membrane (16,17). To also determine the effect of the two Phe residues in the sequence of tritrpticin on the activity, we decided to substitute these by Tyr residues, which would be expected to influence the positioning of the peptide in the membrane. A third change could focus on the cationic residues of tritrpticin. The four cationic residues at the terminal ends of tritrpticin are important for its antibacterial activity because

Submitted March 26, 2006, and accepted for publication August 18, 2006.

Address reprint requests to Dr. Hans J. Vogel, Dept. of Biological Sciences, University of Calgary, Calgary, Alberta, Canada T2N 1N4. Tel.: 403-220-6006; Fax: 403-289-9311; E-mail: vogel@ucalgary.ca.

0006-3495/06/12/4413/14 $2.00

doi: 10.1529/biophysj.106.085837

the removal of even one Arg decreases the activity (11). However, it is not essential that the cationic residues be Arg, as their replacement with Lys is apparently not deleterious to the activity of either tritrpticin or its symmetric variant (11,13).

The NMR structure of indolicidin in dodecylphosphocholine micelles (DPC) was determined to be an extended turn-like structure (18). This is in contrast to the NMR structure of tritrpticin, which formed a compact two-turn amphipathic structure in SDS micelles (10). The two Pro residues of tritrpticin helped form the two turns in this structure, and it would therefore be of interest to replace these two residues with Ala as well. The *cis-trans* proline isomerization observed for tritrpticin in aqueous solution was significantly decreased upon insertion into detergent micelles, inducing the formation of a single major conformer. This X-Pro *cis-trans* isomerization has also been observed for indolicidin, although indolicidin does not form a single conformer in detergent as readily as tritrpticin (D. J. Schibli and H. J. Vogel, unpublished data; (18)). The substitution of Pro, a helix-breaking residue, to Ala, a helix-promoting residue, results in the formation of a continuous α-helical structure for indolicidin in DPC micelles (7) as well as for hCT (9–32), a human calcitonin-derived cell-penetrating peptide (19). Recently, the NMR structures of a number of other short Trp-rich peptides have also been determined; the vast majority form amphipathic structures in detergent micelles, with the Trp residues forming the hydrophobic core of an amphipathic structure (10,20–24).

We have previously investigated the interactions of tritrpticin with large unilamellar vesicles and have observed that both tritrpticin and indolicidin preferentially insert into the membrane/water interface of phospholipid vesicles with negatively charged headgroups (23). In addition, as mentioned above, the solution NMR structure of tritrpticin has also been determined in SDS micelles (10). In this work, we compare a group of eight amidated analogs of tritrpticin (Table 1) in which sets of amino acids have been systematically examined to determine their effects on antimicrobial activity, membrane perturbation properties, and structures in detergent micelles.

TABLE 1 Sequences of the tritrpticin analogs

Peptide	Variant	Sequence
Tritrpticin		VRRFPWWWPFLRR
Tritrp1	NH_2	VRRFPWWWPFLRR-**NH_2**
Tritrp2	R→K	V**KK**FPWWWPFL**KK-NH_2**
Tritrp3	P→A	VRRF**A**WWW**A**FLRR-**NH_2**
Tritrp4	W→Y	VRRFP**YYY**PFLRR-**NH_2**
Tritrp5	F→Y	VRR**Y**PWWWP**Y**LRR-**NH_2**
Tritrp6	W→F	VRRFP**FFF**PFLRR-**NH_2**
Tritrp7	P1→A1	VRRF**A**WWWPFLRR-**NH_2**
Tritrp8	P2→A2	VRRFPWWW**A**FLRR-**NH_2**
Indolicidin		ILPWKWPWWPWRR-**NH_2**

Sequence changes relative to the parent tritrpticin peptide are denoted by bold text.

MATERIALS AND METHODS

Materials and peptide synthesis

All peptides used in this study were synthesized using standard fluoromethoxy carbonyl (fmoc) chemistry. Tritrpticin, indolicidin, and Tritrp6 and 7 were synthesized at the Peptide Synthesis Facility at Queens University (Kingston, Ontario, Canada). Tritrp1–5 were synthesized at the University of Victoria Protein Chemistry Centre (Victoria, British Columbia, Canada) on an Applied Biosystems (Foster State, CA) model 430A peptide synthesizer. Tritrp8 was purchased from AnaSpec (San Jose, CA). All peptides were purified to >95% purity using reverse-phase high-performance liquid chromatography. All lipids, including the fluorophore labeled 1-oleoyl-2-[6-[(7-nitro-2-1,3-benzoxadiazol-4-yl)amino]hexanoyl]-*sn*-glycero-3-phosphocholine lipid (C_6-NBD-PC), were purchased from Avanti Polar Lipids (Alabaster, Ala). Calcein and α-chymotrypsin were purchased from Sigma (St. Louis, MO). All other chemicals were purchased from standard suppliers.

Antimicrobial and hemolytic assays

The antimicrobial activities of the peptides used in this study were assayed using the broth microdilution method by determining both the minimal inhibitory concentration (MIC) and minimal bactericidal concentration (MBC) as described previously (25). Briefly, *Escherichia coli* and *Staphylococcus aureus* strains were grown to the exponential growth phase in 2% Bacto-Peptone media and diluted to 2×10^6 cfu/mL in the wells of a 96-well polystyrene plate. The peptides were diluted between 100 and 1 μg/mL and the cultures were incubated overnight at 37°C. The change in turbidity of the bacteria cultures was monitored at 540 nm with a Microwell System Reader 510 spectrophotometer (Organon Teknika, Boxtel, The Netherlands). The MBC was determined by removing a 10-μL aliquot from the overnight culture and plating on Paper Disk Method antibiotic sensitivity medium II (AB Biodisk, Solna, Sweden) and incubating for a second night at 37°C.

The hemolytic assay was performed using red blood cells from heparinized human blood as previously described (25). Briefly, freshly collected human blood was centrifuged at 1500 rpm for 10 min at 4°C and washed with phosphate buffered saline, pH 7.3. Red blood cells were diluted to 1% and incubated with various peptide dilutions for 1 h at 37°C. Samples were subsequently centrifuged at 4000 rpm for 5 min before the absorbance of the supernatant was measured at 540 nm. A zero hemolysis blank and a measurement of 100% hemolysis (cells lysed by 1% Triton X-100) were also determined. The concentration of peptide required for 50% hemolysis (EC_{50}) was determined from dose-response curves. The antimicrobial and hemolytic assays were both performed at the University Hospital of Trømso (Trømso, Norway).

Calcein leakage

A standard calcein leakage assay (26) was performed to determine the effects of various peptides on the permeability of synthetic large unilamellar vesicles (LUVs). LUVs were prepared using the extrusion method as previously described (20). LUVs were made of lipid mixtures of egg-yolk phosphatidyl choline (ePC), egg-yolk phosphatidyl ethanolamine (ePE), and egg-yolk phosphatidyl glycerol (ePG) in 1:1 ratios for both ePC:ePG and ePE:ePG. Additionally, ePC LUVs containing cholesterol were made with a composition of ePC:cholesterol in a 2.5:1 ratio. Lipid films were formed by mixing phospholipids dissolved in chloroform followed by evaporation of the chloroform under a stream of nitrogen gas. The lipid films were solubilized in leakage buffer (10 mM Tris, 150 mM NaCl, 1 mM EDTA, pH 7.4) and 70 mM calcein. The lipid suspensions were further processed with five cycles of freezing and thawing, followed by a minimum of 11 passes through two stacked 0.1-μm polycarbonate filters (Nucleopore Filtration Products, Pleasanton, CA) using a Mini-Extruder (Avanti Polar Lipids) at room temperature (27,28). After extrusion, free calcein was removed from the LUVs with encapsulated calcein by gel filtration on an 18-cm Sephadex G-50

column equilibrated with leakage buffer. Fractions containing LUVs were determined by light scattering at 400 nm. The phospholipid concentration was determined by assaying lipid phosphorus by the method of Ames (29).

Leakage experiments were performed on a Varian Cary Eclipse fluorimeter with excitation and emission wavelengths of 490 nm and 520 nm, excitation and emission slit widths of 5 nm, and a PMT detector voltage of 400 V. Measurements were carried out in a 2-mL sample volume with mixing and a sample temperature of 37°C using a Peltier temperature control device. Calcein-encapsulated LUVs were diluted in leakage buffer to a final phospholipid concentration of 10 μM. For higher lipid concentrations, LUVs prepared in leakage buffer lacking calcein were added. To induce calcein leakage, peptide was added to a final concentration of 1 μM. The degree of calcein leakage was assessed at peptide to lipid (P/L) ratios of 1:10, 1:20, 1:30, 1:50, 1:100, and 1:200. Using the Kinetics program in the Cary Eclipse software package, the baseline fluorescence was monitored for a minimum of 1–2 min (F_o). After the addition of peptide the increase in fluorescence due to the dilution of the calcein dye (F) was monitored for 10 min or until the fluorescence no longer increased. The total calcein fluorescence (F_T) was determined by the addition of 20 μL of 10% Triton X-100, with the fluorescence monitored for a minimum of 1 min or until the fluorescence readings had stabilized. All values were averaged over 1–10 s and the assays were performed in triplicate. The percent leakage was calculated as follows:

$$\%\text{Leakage} = ((F - F_o)/(F_T - F_o)) \times 100.$$

Lipid flip-flop

Asymmetrically labeled NBD vesicles for lipid flip-flop experiments (23) were made by the extrusion method with an Avanti miniextruder (Avanti Polar Lipids). Vesicles were made using a lipid composition of 1:1:0.005 ePC:ePG:C_6-NBD-PC and solubilized in leakage buffer. After extrusion, the LUVs are symmetrically labeled with the C_6-NBD-PC fluorophore in both leaflets of the bilayer. To produce asymmetrically labeled LUVs, the outer leaflet NBD fluorophores were chemically quenched by incubating the LUVs with 60 mM dithionite (60 μL of 1 M dithionite, 1 M Tris added to 1 mL of LUVs) for 20 min at 30°C. Immediately after this, the dithionite was removed by gel filtration on a Sephadex G-50 column, and fractions containing the asymmetrically labeled LUVs were monitored by light scattering at 400 nm and pooled. The asymmetric NBD labeled LUVs were diluted to 10 μM in 19 mL of leakage buffer and allowed to equilibrate for a minimum of 20 min at 37°C. Before the addition of peptide, a zero time point was obtained to determine background lipid flip-flop. To induce lipid flip-flop, peptides were added to a final concentration of 0.2 μM, giving a peptide/lipid ratio of 1:50. Samples were removed at time points of 30, 60, 120, 300, and 600 s. To stop the flip-flop reaction, samples were immediately mixed with 30 μL of 25 mg/mL α-chymotrypsin and incubated at 30°C for a minimum of 30 min. The NBD fluorescence was monitored on a Varian Cary Eclipse fluorimeter with excitation and emission wavelengths of 460 nm and 537 nm, excitation and emission slit widths of 10 nm, a PMT detector voltage of 600 V, and Savitzky-Golay averaging with a 5-nm filter. Measurements were carried out in a 3-mL sample volume and a sample block temperature of 30°C with mixing. Using the Kinetics software in the Cary Eclipse software package, fluorescence was monitored for a minimum of 2 min or until the NBD fluorescence had equilibrated. The degree of peptide-induced flip-flop of the NBD labeled PC lipid, was determined by the addition of 30 μL of 1 M dithionite, 1 M Tris. The decrease in fluorescence was monitored over time until the fluorescence had equilibrated (5–20 min). To determine the background fluorescence, the LUVs were disrupted by the addition of 15 μL of 20% Triton X-100, and the remaining NBD-labeled lipids were quenched by dithionite. The background fluorescence was monitored for ~2 min or until the baseline had stabilized. The percent flip-flop was calculated as follows:

$$\%\text{flip-flop} = (100 - ((F - F_{bkg})/(F_o - F_{bkg})) \times 100),$$

where F is the average fluorescence after complete quenching of any flipped lipids (usually measured at 20 min after the addition of dithionite), F_{bkg} is the average fluorescence after the addition of Triton X-100, and F_o is the average fluorescence before the addition of peptide. To remove variability, all fluorescence values represent the average fluorescence over 20 data points. To remove any effect of the dithionite/Tris solution, the percentage of flip-flop in the absence of peptide at the same time measured for F in the presence of peptide was subtracted from the percentage of flip-flop in the presence of peptide. The assays were performed in triplicate.

NMR experiments

NMR samples for each peptide were prepared by dissolving ~3–5 mg of peptide in 9:1 H_2O:D_2O; DSS was added as an internal chemical shift reference. One-dimensional (1D) ^{1}H spectra were first acquired for the peptide in aqueous solution. The peptides were then solubilized in DPC-d_{38} at ~1:100 of peptide/DPC to ensure one peptide molecule per detergent micelle. No change in linewidth was observed when the ratio of peptide to detergent was varied, suggesting that there is no contribution of peptide oligomerization. More detailed studies of peptide oligomerization upon binding to membrane mimetics would require studies with fluorescence resonance energy transfer.

All NMR spectra were acquired on either a Bruker Avance 500 MHz NMR spectrometer equipped with a Cryo-Probe or a Bruker Avance 700 MHz Ultrashield NMR spectrometer (Bio-NMR Centre, University of Calgary, Calgary, Alberta, Canada). All spectra were referenced to 2,2-dimethyl-2-silapentane-5-sulfonic acid (DSS). The mixing time for all nuclear Overhauser enhancement and exchange spectroscopy (NOESY) spectra was 100 ms and 60 ms for all total correlation spectroscopy (TOCSY) spectra. Water suppression was performed using an excitation sculpting pulse sequence for all TOCSY and NOESY spectra (30) and a Watergate 3-9-19 pulse sequence (31) for the correlation spectroscopy (COSY) spectra. Spectra were processed using NMRPipe (32) on a PC workstation running Redhat Linux 7.3. All spectra were zero-filled and multiplied by a shifted sine-bell curve before Fourier transformation of the free induction decay (FID). To determine if there were any slowly exchanging amide protons, a deuterium amide exchange experiment was performed by dissolving a lyophilized NMR sample in 99.9% D_2O and immediately obtaining one-dimensional ^{1}H NMR spectra at different time intervals.

Structure calculation

Chemical shift assignment and nuclear Overhauser enhancement (NOE) peak list generation were performed using the NMRView 4.1.3 software package (33) on a PC workstation running the Redhat 7.3 version of the Linux operating system. The assignment of the chemical shifts was determined using the method of Wüthrich (34). Where possible, stereospecific assignments were made for well-resolved proton signals, such as the tryptophan and proline rings. All structure calculations were performed using ARIA 1.1.2 (35–38). ARIA enables the incorporation of ambiguous NOE distance restraints into the structure calculations, as well as calibrating the NOE distance restraints using a structure-based NOE back calculation. For non-Pro residues, a broad dihedral angle restraint was used in the structure calculations to restrain the ϕ-dihedral angle between $-35°$ and $-175°$. Each ARIA run was performed with nine iterations, using the default parameters supplied in the program. Peak lists that were compatible with ARIA were generated by NMRView. In the final ARIA run, the number of structures generated in the final iteration was increased to 100 while 20 structures were retained based on lowest energy.

RESULTS

Antimicrobial assays

A standard microdilution method (25) was used to determine both the minimal inhibitory concentration (MIC) and the

minimal bactericidal concentration (MBC) for tritrpticin and eight analogs of tritrpticin (Table 2). Due to the similarity in amino acid composition between indolicidin and tritrpticin and the thorough studies of this peptide reported in the literature, indolicidin was included as a reference peptide. In this study, the antimicrobial activities of tritrpticin and indolicidin were found to be very similar, as has been previously observed (11). All of the peptides appear to be approximately twofold more active against the Gram positive *S. aureus* bacteria compared to the Gram negative *E. coli*, agreeing with previous reports for both tritrpticin and indolicidin (4,5,8,39).

The removal of the negative charge on the C-terminus by amidation increases the net positive charge of a peptide, which is generally observed to increase the antimicrobial activity of antimicrobial peptides. The amidated tritrpticin peptide, Tritrp1, has an approximately twofold greater activity than the parent tritrpticin peptide (Table 2). As all of the remaining tritrpticin analogs used in this study also have an amidated C-terminus, the activity of all of the peptides are subsequently compared to Tritrp1. In general, there are very few significant differences in the antimicrobial activity of any of these peptides, with Tritrp2, 3, 5, 6, and 7 all having similar MIC and MBC values against *E. coli* compared to Tritrp1 and tritrpticin. The only peptide in this study that had a significant loss in activity against both *E. coli* and *S. aureus* was Tritrp4, which had 5- to 10-fold less activity against *E. coli* and 2.5- to 5-fold less activity against *S. aureus*. The results observed for Tritrp6 and 8 are also interesting; whereas the MIC values do not appear to be very different from Tritrp1 for either *E. coli* or *S. aureus*, the MBC values against *E. coli* increase ~2- to 2.5-fold in relation to Tritrp1 and the MBC values against *S. aureus* remain similar, suggesting that the variations of the Trp to Phe or the second Pro to Ala may increase the selectivity for killing Gram positive bacteria.

Because the major requirement for an antibiotic is for it to be selective for microbes versus human cells, the efficacy of an antimicrobial peptide must be determined by comparing the antimicrobial and hemolytic activities (HA) for a given peptide (Table 2). This can best be visualized by calculating the therapeutic index for a peptide (Table 3), the ratio of its hemolytic activity to either its MIC or MBC (HA/MIC or HA/MBC). The selective nature of antimicrobial peptides has long been attributed to the differences in the membrane compositions of the outer leaflets of mammalian cells (these commonly have neutral zwitterionic phospholipids headgroups) and microbial cells (that normally have a net negative charge on their surface) (40). Therefore, it would be expected that increasing the net positive charge of a peptide by amidating the C-terminus should not only increase the antimicrobial activity by removing the repulsion with the phosphodiester groups, but also improve the selectivity of the peptide for microbial cells. As mentioned above, the increase in the net positive charge by amidating the C-terminus slightly increases the antimicrobial activity of tritrpticin, but there is also a corresponding increase in the hemolytic activity (Table 2). This suggests that the presence or absence of the negative charge may not improve the antimicrobial selectivity of tritrpticin. There are four peptides in this study that do not appear to cause any significant hemolysis of red blood cells, Tritrp2, 4, 6, and 7 (Table 2). Of these peptides, the Trp to Tyr replacement in Tritrp4 results in a general loss of activity (Tables 2 and 3). On the other hand, the replacement of the four Arg by Lys (Tritrp2), the replacement of the three central Trps by Phe (Tritrp6), or the single replacement of the first Pro at position 5 in tritrpticin by Ala (Tritrp7) do not cause any significant loss in antimicrobial activity, exemplified by their high therapeutic index (Table 3). The related nonamidated versions of Tritrp2 and Tritrp6 demonstrated similar decreases in hemolysis without any significant loss in antimicrobial activity (12,13). The substitution of Pro-5 to Ala in Tritrp7 results in a major loss in hemolytic activity compared to Tritrp1, but the substitution of Pro-9 to Ala in Tritrp8 gives roughly half the hemolytic activity of Tritrp1. The dual proline substitutions in Tritrp3 has an approximately threefold higher hemolytic activity than Tritrp1, making it the peptide with the lowest therapeutic index value in this study despite being highly antimicrobial.

TABLE 2 Antimicrobial and hemolytic activity of peptides used in this study

		MIC (μg/mL)		MBC (μg/mL)		Hemolysis
Peptide	Variant	*E. coli*	*S. aureus*	*E. coli*	*S. aureus*	EC_{50} (μg/mL)
Tritrpticin	–	20	10–20	20	20	380
Tritrp1	NH_2	10-20	<2.5–5	10–20	10	190
Tritrp2	R→K	20	10	20	10	>1000
Tritrp3	P→A	10	5	10	10	60
Tritrp4	W→Y	50	20–25	100	25	>1000
Tritrp5	F→Y	20	5	20	10	220
Tritrp6	W→F	20	6	40	8	>1000
Tritrp7	P1→A1	20	4	20	7	>1000
Tritrp8	P2→A2	20	5	40	17.5	354
Indolicidin	–	20	10	20	10	310

TABLE 3 Therapeutic index for the tritrpticin analogs

		Therapeutic index			
		(Hemolysis/MIC)		(Hemolysis/MBC)	
Peptide	Variant	*E. coli*	*S. aureus*	*E. coli*	*S. aureus*
Tritrpticin	–	19	25	19	19
Tritrp1	NH_2	13	51	13	19
Tritrp2	R→K	50	100	50	100
Tritrp3	P→A	6	12	6	6
Tritrp4	W→Y	20	44	10	40
Tritrp5	F→Y	11	44	11	22
Tritrp6	W→F	50	167	25	125
Tritrp7	P1→A1	50	250	50	143
Tritrp8	P2→A2	18	71	9	20
Indolicidin	–	15	31	15	31

Calcein leakage

Leakage of the contents of phospholipid liposomes by antimicrobial peptides has often been assumed to be the result of pore formation and is thought to be related to the lysis of bacterial membranes (23,41). We have examined the leakage profiles of the tritrpticin analogs in anionic vesicles, made up of two phospholipid compositions, ePC:ePG (1:1) and ePE:ePG (1:1) (Fig. 1). In the ePC:ePG LUVs (Fig. 1 *A*) there is a clear distribution between those peptides that cause high leakage (>60% at P/L of 1:10; tritrp1, 2, 3, 5, 7, 8, and tritrpticin) and those that induce lower leakage (<40% at P/L of 1:10; Tritrp4, 6, and indolicidin). With the exceptions of Tritrp7 and the peptides that cause low overall leakage, the maximum percentage leakage appears to be reached at a P/L ratio of 1:20 in the ePC:ePG LUVs. It is interesting to note that Tritrp7(P1→A1) has a different leakage dose-response profile compared to the other peptides that cause high leakage; instead of having a sigmoidal dose-response curve, leakage appears to be much more linear in the range of P/L ratios tested and may not yet have reached its maximal leakage at the highest P/L ratio. This is similar to the pattern of the peptides that induce low leakage, where the percentage leakage is slowly increasing in a linear manner in the range of P/L ratios assayed. The leakage profiles observed for Tritrp2 also deviate from the majority of the peptides. Although most of these peptides reach a maximal percentage leakage 2 min after the addition of peptide, the kinetics for the leakage induced by Tritrp2 appear to be quite a bit slower, with the majority of leakage occurring only after ~5–10 min (Fig. 1 *B*). To verify the validity of the 10-min assays, similar assays were also performed for as long as 7 h. The results show that after 10 min, close to maximal leakage has already occurred (data not shown).

In general, those peptides that induced high leakage in the ePC:ePG LUVs (Fig. 1 *A*) also induced high leakage in the ePE:ePG LUVs (Fig. 1 *C*). In the case of the ''high leakers'', the percent leakage at a P/L ratio of 1:10 is generally as high as was observed in the ePC:ePG LUVs or in the case of

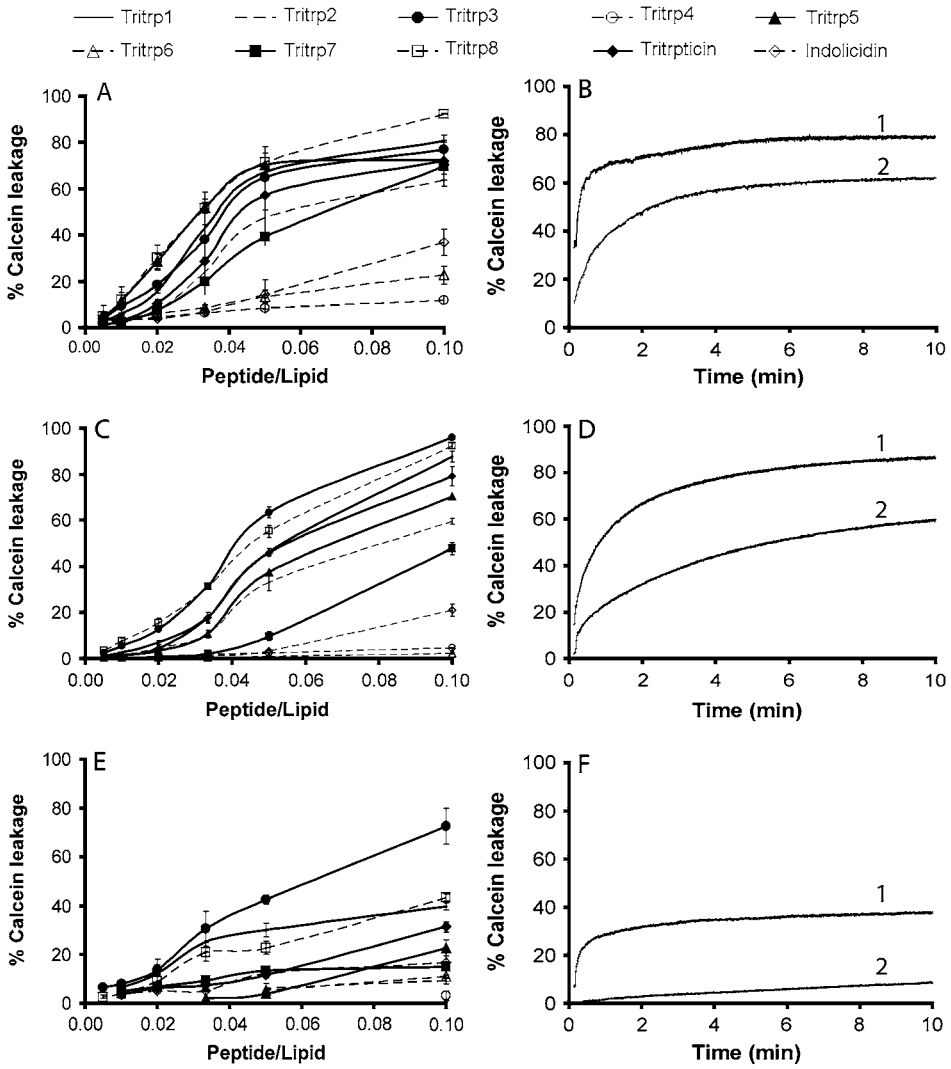

FIGURE 1 Induction of calcein leakage from LUVs for the Tritrp analogs. Summary of leakage experiments done in triplicate from (*A*) 1:1 ePC:ePG, (*C*) 1:1 ePE:ePG LUVs, and (*E*) 2.5:1 ePC:cholesterol. Sample calcein leakage profiles in (*B*) ePC:ePG, (*D*) ePE:ePG, and (*F*) ePC:cholesterol for Tritrp1 (*trace 1*) and Tritrp2 (*trace 2*). The leakage profile of Tritrp1 is representative of all of the peptides, except for Tritrp2, that cause significant leakage. The initial leakage event occurs significantly faster for Tritrp1 than for the Tritrp2 peptide in all of the vesicle systems studied here. All sample traces were taken for a peptide to lipid ratio of 1:10.

Tritrp1 and 3 the percent leakage surpasses the percent leakage observed in the ePC:ePG LUVs, nearing 100%. It should be noted that in the concentration range tested it is not certain if the maximal leakage occurred for any of the peptides in ePE:ePG LUVs. The peptides that induced low leakage in the ePC:ePG LUVs (Tritrp4, 6, and indolicidin) induced even lower leakage in the ePE:ePG LUVs; this was especially apparent for Tritrp4 and 6, the two analogs in which the three Trp residues have been replaced by either Tyr or Phe. As in the ePC:ePG LUVs, Tritrp7 is also an exception in the ePE containing LUVs. For this peptide, significant leakage occurs at much higher P/L ratios than the other ''high leakers'', but at a P/L of 1:10, the final percent leakage is much higher than the ''low leakers'', coming very close to the ''high leakers''. The slow leakage kinetics mentioned above for Tritrp2 also occurs in the ePE:ePG LUVs, although the difference between Tritrp2 and the other peptides is not as acute due to the slower leakage kinetics observed for the other ''high leakers'' (Fig. 1 *D*).

In addition to determining the percent leakage from anionic LUVs, calcein leakage from neutral vesicles composed of egg-yolk phosphatidylcholine and cholesterol (ePC:cholesterol 2.5:1) were also assayed (Fig. 1 *E*). It is interesting that all of the tritrpticin analogs that had induced low hemolysis (Tritrp2, 4, 6 and 7) also give rise to very low leakage from the neutral LUVs at high P/L ratios (i.e., 1:10). This was not unexpected for Tritrp4 and 6, which did not cause significant leakage in either of the anionic LUVs at these concentrations. However, Tritrp2 and Tritrp7 both caused significant leakage from both ePC:ePG and ePE:ePG LUVs at P/L ratios of 1:10. The most hemolytic peptide, Tritrp3, also induced the most leakage from the ePC:cholesterol LUVs. The remaining peptides (tritrpticin, indolicidin, and Tritrp1, 5, and 8) induced both intermediate leakage and intermediate hemolysis.

Lipid flip-flop

One of the mechanisms proposed to explain the membrane-perturbing action of antimicrobial peptides is the formation of ''toroidal pores'', comprised of peptides and lipids, on the negatively charged bacterial membranes (41,42). To determine whether tritrpticin and its related analogs are capable of forming toroidal pores, the degree of phospholipid flip-flop was measured using vesicles asymmetrically labeled with an NBD-labeled phosphatidylcholine lipid. A P/L ratio of 1:50 was used in these experiments since maximum leakage had not yet been reached at this ratio in the calcein leakage experiments with the ePC:ePG LUVs and it was expected that differences in flip-flop would be more pronounced at this ratio. It is assumed that the maximum flip-flop should be ~50% since after complete mixing of the two leaflets there is an equal probability of finding an NBD-PC lipid in the inner or outer leaflet, although this assumes that vesicle integrity is retained during the reaction. All of the analogs studied here induced lipid flip-flop to some degree in a time-dependent fashion at a P/L of 1:50 (Fig. 2 *A*). The triplicates of these assays resulted in the same relative percent flip-flop values between the peptides. The peptides can be grouped in relation to the degree to which they induced lipid flip-flop. Those peptides that induced low flip-flop (<10% flip-flop) included Tritrp2, 4, 6, and indolicidin. Those peptides that induced medium flip-flop (<20% flip-flop) included Tritrp7 and tritrpticin while those that induced the highest flip-flop (>20% flip-flop) included Tritrp1, 3, 5, and 8. The capacity to induce lipid flip-flop correlates with the degree to which the peptides caused calcein leakage from ePC:ePG LUVs at the same P/L (Fig. 2 *B*), suggesting that lipid flip-flop is part of the mechanism that gives rise to peptide-induced contents leakage in phospholipid vesicles. It should be noted that while the data for Tritrp2 and Tritrp7 would suggest that they do not cause significant lipid flip-flop, this could be the result of the P/L used, since at higher ratios, such as 1:10, these analogs caused higher levels of calcein leakage in ePC:ePG LUVs, equal to that observed with the other, more active peptides (Fig. 1 *A*).

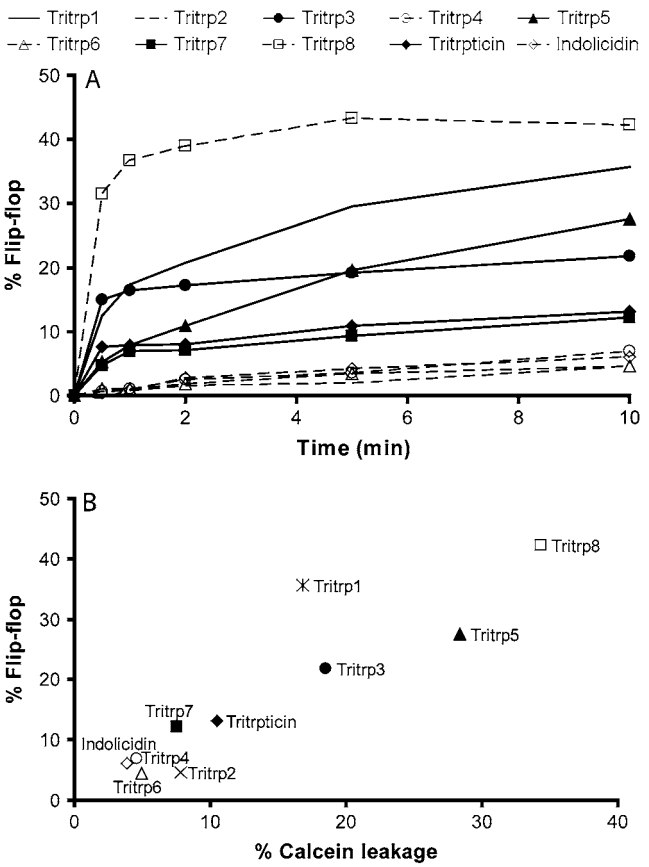

FIGURE 2 Phospholipid flip-flop induced by the Tritrp analogs. (*A*) Percent lipid flip-flop from ePC:ePG:NBD-PC 1:1:0.005 LUVs. (*B*) Correlation between calcein leakage and lipid flip-flop from ePC:ePG LUVs at a peptide to lipid ratio of 1:50, taken after 10 min.

NMR spectroscopy and structure determination

DPC micelles were chosen as a membrane mimetic for NMR studies due to their structural similarity to phospholipids, including the presence of an interfacial phosphodiester group and a choline headgroup. Previous experiments with tritrpticin (43), have demonstrated that the tryptophan fluorescence of peptides in DPC micelles is similar to the tryptophan fluorescence observed in phospholipid vesicles. Additionally, the fluorescence and CD spectra of both indolicidin and its analog, CP10A, in DPC micelles was very similar to that observed in POPC LUVs (7). A further motivation for using DPC rather than SDS in these studies is that there was significant chemical shift overlap for the original tritrpticin peptide in SDS micelles (10), which was significantly reduced in DPC micelles. Initial studies with the Tritrp1 and Tritrp3 analogs demonstrated much better resolved spectra at 37°C than at 25°C, therefore the NMR spectra for the remaining peptides were acquired at 37°C.

As previously observed for the parent tritrpticin peptide (10), the free peptides in aqueous solution contained multiple structural conformers. This is most likely due to *cis-trans* proline isomerization, a common phenomenon in linear unstructured peptides. This is most clearly evident by examining the tryptophan indole Hε1 region of the 1D ^{1}H NMR spectra (Fig. 3). In the 1D NMR spectra, the analogs that retained the three central Trp residues and the two flanking Pro residues (Tritrp1, 2, and 5) had ~9–12 peaks present in the Trp Hε1 region when dissolved in water alone. These likely represent the four conformers that would be present due to proline isomerization, likely in decreasing concentrations related to their energetic stability (*trans-trans* > *trans-cis, cis-trans* ≫ *cis-cis*). The presence of only nine signals is probably due to *cis-cis* being in very low abundance and/or signal overlap. Upon insertion of the peptides into DPC micelles, the multiple conformers collapse into a single major conformer (~95%), representing the energetically more favorable *trans-trans* conformation (see below). The confirmation that this structural heterogeneity was most likely due to *cis-trans* proline isomerization can be obtained when examining the 1D-^{1}H spectra of the three proline to alanine analogs (Tritrp3, 7, and 8). Tritrp3 has only a single conformer (only 3 Trp Hε1 signals) in both aqueous solution and when inserted in DPC micelles. Simultaneously, Tritrp7 and 8, the single Pro to Ala analogs, have one major conformer,

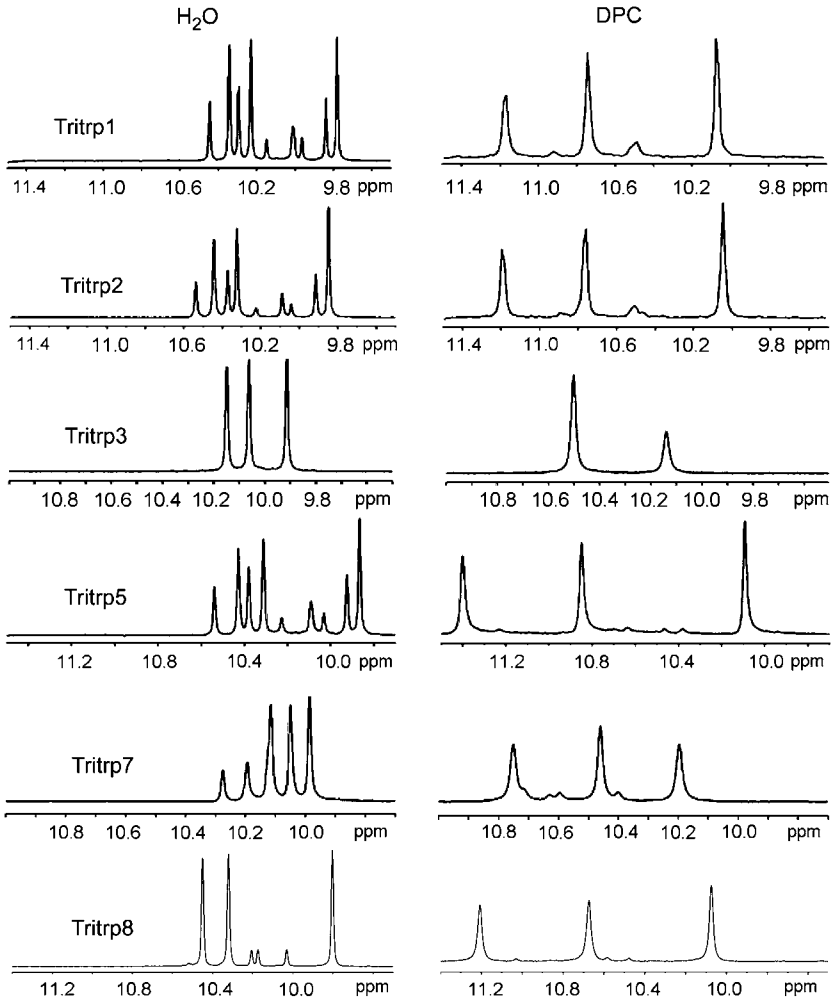

FIGURE 3 One-dimensional proton spectra of the Hε1-tryptophan region for different tritrpticin analogs in aqueous solution and DPC micelles. All of the tryptophan containing analogs used in this study have three Trp residues, therefore if a single structure is present, only three signals should be observed. It should be noted that for Tritrp3, the large signal in DPC micelles is due to two overlapping signals (as determined by 2D NMR spectra).

which is intensified upon insertion into DPC micelles, and a single minor conformer due to the lone Pro residue. An interesting observation is that in the minor conformer for Tritrp7 in DPC micelles, one of the Trp residues has two Hε1 signals, possibly due to two stable backbone conformations of this residue or two different rotameric states of its indole side chain. The remaining two peptides, Tritrp4 and Tritrp6, do not contain Trp residues, and therefore do not contain distinctive signals that can be used to observe multiple conformations. However, upon comparing the fingerprint amide-α crosspeak region in the HSQC spectra of these two peptides in DPC micelles to that of Tritrp1, it is clear that although a major conformer is present, it is not in as high a concentration as compared to the Trp-containing peptides (Fig. 4). The lower concentration of a major conformer and the presence of at least two other minor conformers in the two-dimensional (2D) spectra of Tritrp4 and 6 in the presence of DPC micelles severely complicates the NMR assignment and subsequent structure calculations. One of the backbone amide protons from the Tritrp6 NOESY has a remarkable chemical shift of 8.7 ppm, most likely due to ring current effects in this highly aromatic peptide. It was therefore decided not to pursue NMR structures of these two peptides.

While the peptides examined here are quite short (13 residues), the line broadening due to the DPC detergent resulted in significant signal overlap for the five aromatic residues for many of the peptides. Fortunately, the sequence similarity between the six peptides helped us to resolve spectral overlap issues. In general, the chemical shift assignments of the five peptides were very similar and could be used to confirm difficult assignments in other peptides (Supplementary Material). In particular, those residues that were packed near the indole rings of the Trp residues had very distinctive chemical shifts due to ring-current shifts, most notable were the HB2 and HG2 protons of Pro5, the indole HD1 ring proton of Trp-7 and the amide proton of Trp-7 (Supplementary Material). Where possible, stereospecific assignments were determined from distinctive NOE patterns for the side-chain protons of the Pro residues. Additionally, all of the Pro residues were determined to be in the *trans* conformation based on NOE patterns, specifically strong NOEs between the proline δ-protons and the α- and β-protons of the preceding residue, as well as the absence of strong NOEs between the proline α-proton and the preceding α- and β-protons.

A deuterium exchange experiment was performed for each of the peptides to determine if any of the backbone amides were involved in stable hydrogen bonds. The only peptide that retained any amide signals immediately after becoming solubilized in D_2O was Tritrp3. The amide signals of Trp-8, Phe-10, and Leu-11 remained for ~30 min after the addition of D_2O. Due to chemical shift overlap with the aromatic protons, it was not possible to determine if the other C-terminal amide protons (Trp-7, Ala-9, Arg-12, and Arg-13) also had decreased exchange rates.

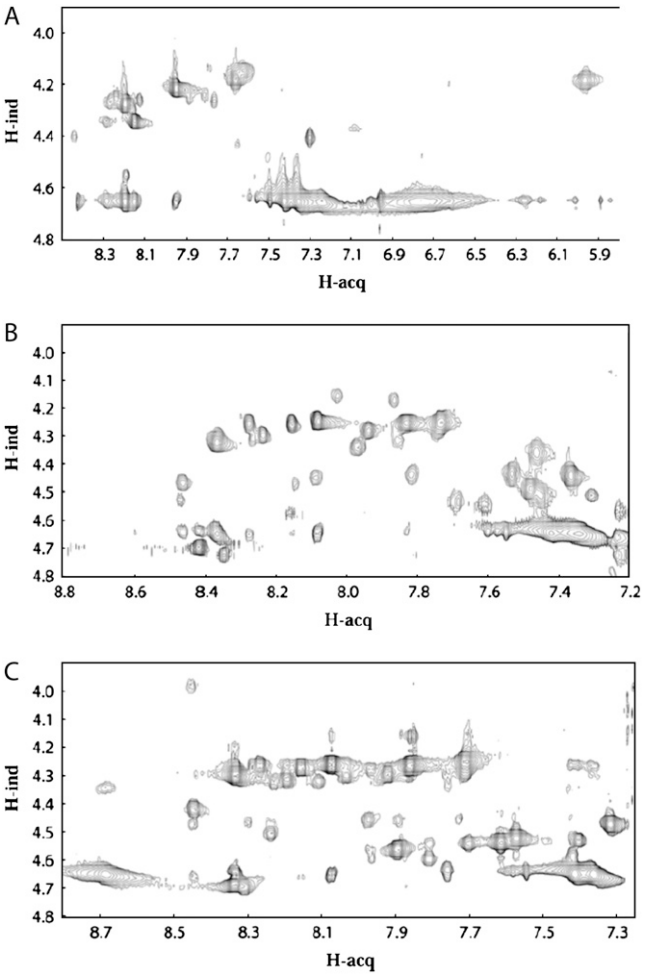

FIGURE 4 Two-dimensional TOCSY spectra of the Tritrp analogs that have the three central tryptophan residues replaced by alternative aromatic amino acids. (*A*) Tritrp1, (*B*) Tritrp4, and (*C*) Tritrp6 in DPC micelles, demonstrating the structural inhomogeneity observed for tritrpticin analogs that lack Trp residues. For each of these 13 residue peptides, a maximum of 10 amide-α resonances should be observed. In Tritrp1, there are ~10 resonances that correspond to the major conformer, and a few very weak signals that are due to the presence of a minor conformer. However, there are at least 30 signals present in the spectra for Tritrp4 and 6, implying a minimum of three separate structures in solution. The multiple conformers are most probably the result of *cis-trans* proline isomerization and are likely more prevalent in Tritrp4 and 6 due to the absence of the membrane-anchoring Trp residues. The peaks at ~4.65 ppm are the result of the NMR signal from water. Spectra were acquired on a 500-MHz Avance Bruker NMR spectrometer.

The Tritrp analog structures were determined using the automated NMR assignment and structure calculation program, ARIA (35–38). For each of the six structures determined, NOEs were determined from a NOESY spectrum obtained at a NMR ^1H frequency of 700 MHz. Additionally, NOEs were also obtained from D_2O NOESY spectra collected at either 700 or 500 MHz. Where possible, NOEs were assigned based on unambiguous chemical shift assignments or on the most logical assignment from the previous ARIA

run. Due to the chemical shift overlap present in the spectra for all of the peptides, ambiguous NOEs were also incorporated and assigned by ARIA. Although, the deuterium exchange results suggest that Trp-8, Phe-10, and Leu-11 of Tritrp3 are present in hydrogen bonds, no hydrogen bond restraints were incorporated in the structure calculations due to their rapid exchange with deuterium. In the final ARIA run, 100 structures were calculated in the ninth iteration and of these, the 20 structures with the lowest energy were retained (Fig. 5). The statistics for the final structures are detailed in Tables 4 and 5.

The NMR solution structures of the six peptides for which structures could be calculated can be classified into two different groups based on their backbone RMSD (Table 5) and secondary structure (Fig. 6). The first group has a turn-turn structure, resembling the initial tritrpticin structure (10) and includes Tritrp1, 2, 5, and 8. These four peptides retain the proline at position 5 and are characterized by an extended N-terminus, followed by two successive turns (Fig. 6). Pro-5 induces a β-turn made up of residues 5–8. This turn is likely stabilized by a hydrogen bond between the carbonyl of Pro-5 and the amide proton of Trp-8, which is calculated to occur in more than half of the structures determined for this class of peptide. A specific restraint was not incorporated into the structure calculations for this hydrogen bond and therefore it does not occur in all of the structures. In structures where it is not formed, it is due to a 180° rotation of the carbonyl of Pro-5; although the remainder of the structures are not significantly altered by this rotation. The first β-turn most closely resembles a Type IV turn, based on the ϕ and ψ angles of Trp-6 and Trp-7 (using the structures that have a hydrogen bond between residues 5 and 8). After this first β-turn, there is a short single turn of α-helix between residues 8 and 12 for Tritrp1, 2, and 5. In the final 20 structures of Tritrp8, this second turn is not fully α-helical.

Aside from the turn-turn or turn-helix secondary structure, these four structures are also characterized by a similar clustering of their three tryptophan indole rings (Fig. 6). The indole rings of Trp-6 and Trp-7 are perpendicular to each other and the indole ring of Trp-8 lies somewhat parallel to the ring of Trp-7. These interactions, as well as the clustering of the remaining two aromatic side chains (Phe or Tyr), and

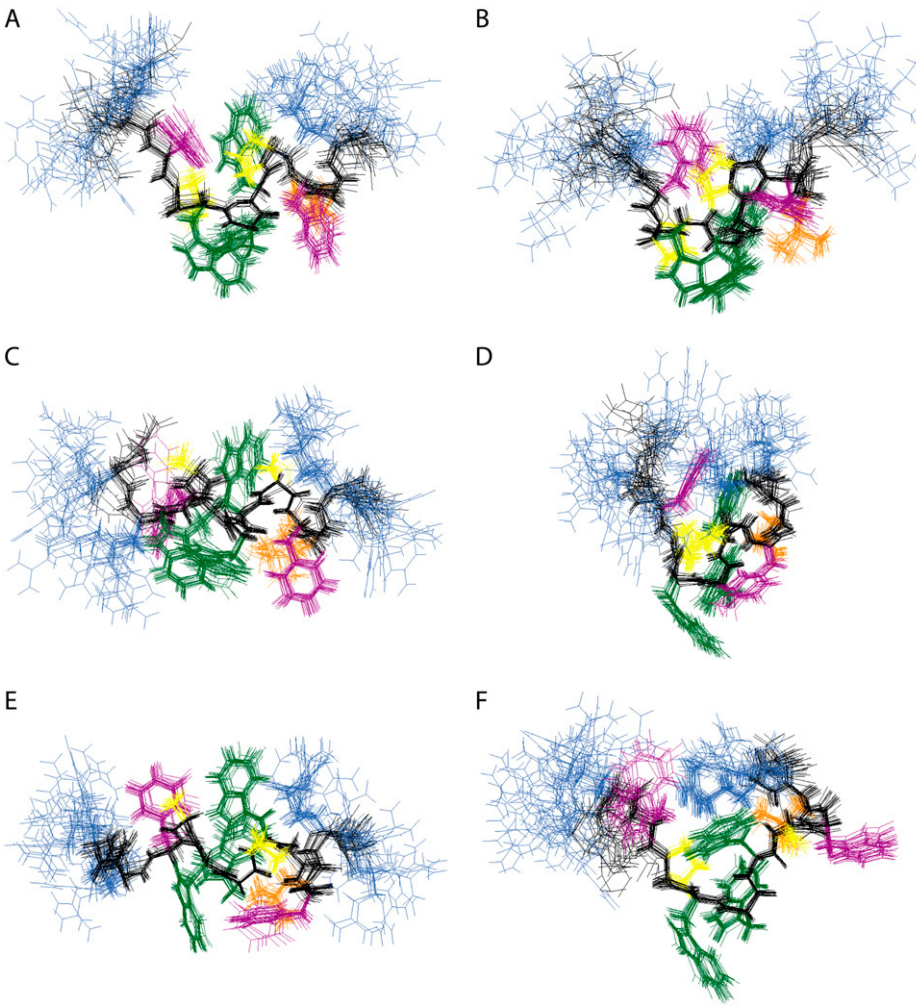

FIGURE 5 The 20 lowest energy structures from the 100 structures calculated in the final iteration of ARIA for the Tritrp analogs in DPC micelles. (*A*) Tritrp1, (*B*) Tritrp2, (*C*) Tritrp3, (*D*) Tritrp5, (*E*) Tritrp7, and (*F*) Tritrp8. All structures are overlaid for all heavy atoms for residues 3–12; the RMSD values for the different structures is presented in Table 5. The backbone of all structures is shown in black, while the side chains of the Trp residues are displayed in dark green, the Phe or Tyr residues in dark violet, the Pro and/or Ala residues in yellow, the Leu residue in dark orange, and the Lys or Arg residues in blue.

TABLE 4 Structural statistics for the final NMR structures

	Tritrp1	Tritrp2	Tritrp3	Tritrp5	Tritrp7	Tritrp8
No. of distance restraints*						
Unambiguous NOEs	514	436	410	494	458	432
Ambiguous NOEs	40	43	32	51	51	9
Total NOEs	554	479	442	545	509	441
Intraresidue NOEs	235	208	174	242	205	217
Sequential NOEs	147	118	122	131	143	131
Medium range NOEs	124	106	95	108	100	71
Long range NOEs	48	47	51	64	61	52
Broad dihedral restraints	10	10	12	10	11	11
RMS distances from ideal values						
Bonds (Å)	$1.0 \times 10^{-2} \pm 4.0 \times 10^{-4}$	$7.6 \times 10^{-3} \pm 6.0 \times 10^{-4}$	$7.0 \times 10^{-3} \pm 4.7 \times 10^{-5}$	$7.36 \times 10^{-3} \pm 1.1 \times 10^{-4}$	$9.4 \times 10^{-3} \pm 4.2 \times 10^{-4}$	$1.86 \times 10^{-3} \pm 6.38 \times 10^{-5}$
Angles (°)	$0.94 \pm 3.2 \times 10^{-2}$	$0.91 \pm 7.9 \times 10^{-2}$	$0.69 \pm 4.3 \times 10^{-3}$	$0.62 \pm 1.6 \times 10^{-2}$	$0.79 \pm 3.3 \times 10^{-2}$	$0.43 \pm 1.37 \times 10^{-2}$
Impropers (°)	$0.75 \pm 6.8 \times 10^{-2}$	$0.70 \pm 8.8 \times 10^{-2}$	$0.58 \pm 1.3 \times 10^{-2}$	$0.53 \pm 1.4 \times 10^{-2}$	$0.53 \pm 3.7 \times 10^{-2}$	$0.33 \pm 1.18 \times 10^{-2}$
Van der Waals (kcal/mol)	81.5 ± 4.2	70.5 ± 6.1	67.0 ± 1.9	52 ± 1.0	85 ± 6.4	20.6 ± 1.2
Distance restraints						
Unambiguous (Å)	$0.24 \pm 1.7 \times 10^{-2}$	$0.38 \pm 2.5 \times 10^{-2}$	$0.14 \pm 3.9 \times 10^{-2}$	$0.30 \pm 1.0 \times 10^{-3}$	$0.25 \pm 4.8 \times 10^{-2}$	$1.25 \times 10^{-2} \pm 7.12 \times 10^{-4}$
Ambiguous (Å)	0	$8.0 \times 10^{-3} \pm 1.0 \times 10^{-2}$	$0.21 \pm 3.0 \times 10^{-3}$	$8.2 \times 10^{-3} \pm 1.3 \times 10^{-2}$	$0.15 \pm 7.1 \times 10^{-2}$	0
All distance restraints (Å)	$0.23 \pm 1.6 \times 10^{-2}$	$0.36 \pm 2.5 \times 10^{-2}$	$0.15 \pm 3.3 \times 10^{-2}$	$0.29 \pm 1.0 \times 10^{-2}$	$0.24 \pm 4.5 \times 10^{-2}$	$1.23 \times 10^{-2} \pm 7.05 \times 10^{-4}$
Dihedral restraints (°)	0	1.49 ± 0.37	$2.27 \pm 6.2 \times 10^{-2}$	0	0.35 ± 0.19	$1.09 \times 10^{-2} \pm 2.00 \times 10^{-2}$
Nonbonded energies						
Total Energy	−183 ± 48	−300 ± 85	−235 ± 99	−263 ± 66	−243 ± 58	−199 ± 16
Electronic (kcal/mol)	−243 ± 61	−342 ± 86	−225 ± 96	−249 ± 64	−267 ± 63	−160 ± 17
Van der Waals (kcal/mol)	−111 ± 26	−104 ± 24	−104 ± 42.7	−118 ± 27	−118 ± 27	−117 ± 0.93
Global RMSDs						
Backbone (Å)	0.963	1.00	0.465	0.986	0.313	0.579
Heavy atom (Å)	1.730	1.593	1.337	1.951	1.220	1.233
Ramachandran† (%)						
Most favored	60	54	79	67	39	46
Additionally allowed	16	23	8	25	46	26
Generously allowed	23	23	13	8	15	28
Disallowed	1	0	0	0	0	0

*Final data from the final ARIA iteration.
†As determined by Procheck.

the aliphatic side chain of Leu-11, form a distinctive hydrophobic face (Fig. 6). Additionally, while the four cationic residues (either arginine or lysine) are localized to the termini of the peptide, the turn-turn structure brings the N- and C-termini together, forming compact amphipathic structures (Fig. 5). The structures can be confirmed by the unique ring current shifts mentioned above. In Tritrp1, 2, 5, and 8 the downfield shifted HB2 and HG2 protons of Pro-5 and the amide proton of Trp-7 are sandwiched between the indole rings of Trp-6 and Trp-7, while the corresponding HB1 and HG1 protons of Pro-5, which are not significantly shifted from their expected values (33), are facing away from the indole rings (Fig. 6).

Tritrp3 and Tritrp7 make up the second class, and are characterized by more helical structures (Fig. 6). The replacement of both prolines by alanine in Tritrp3 induces a well-defined helix to form for residues 4–11. Tritrp3 was the only peptide studied for which the amide protons were not immediately exchanged with deuterium after the addition of D_2O, supporting the presence of hydrogen bonds in the helical structure. This is similar to what has been reported for the related Pro to Ala analog of indolicidin, CP10A (7). Tritrp7 also forms a helix-like structure from Phe-4 to Leu-11, but the rigidity of Pro-9 and its lack of an amide proton results in a disruption of the helical bonding pattern required for a perfect helix. The largest disruption in the helix occurs between Trp-7 and Ala-5, with an average ψ angle of 55° for Ala-5, likely due to the lack of a hydrogen bond donor at position $i + 4$ from Ala-5. But even with this alteration in the hydrogen bonding pattern, the N-terminus

TABLE 5 Intramolecular backbone and heavy atom RMSD values and the intermolecular backbone RMSD values for residues 3–12 of the calculated peptide structures

	Backbone RMSD for residues 3–12 (Å)					
	1	2	3	5	7	8
1	0.279					
2	0.689	0.325				
3	1.103	1.241	0.192			
5	0.708	0.509	1.277	0.274		
7	1.336	1.474	0.786	1.479	0.185	
8	1.210	1.004	1.483	0.958	1.434	0.184
	Heavy atom RMSD for residues 3–12 (Å)					
	0.894	0.787	0.936	1.005	0.846	0.835

of the structure still resembles the helix observed for Tritrp3. The helical nature of these two peptides results in a more extended structure, with increased separation between the N- and C-termini from what is observed in the turn-turn class of peptides, altering the amphipathic nature of the peptides (Fig. 5). Instead of all four cationic residues clustered together on the ''top'' of the structure, the positive charges are localized to the ends of the peptides. Even with the segregation of the basic residues, the amphipathic nature of the peptide is retained, where the short alanine side chain(s) result in a significantly less hydrophobic surface than the opposing face that includes the aromatic and Leu side chains. The side chain of alanine can be considered intermediate in hydrophobicity, although this is dependent on the hydrophobicity scale used (16,17). It may be energetically favorable to have this side chain facing the solvent if these peptides are inserted in the interfacial region of a phospholipid bilayer.

One significant difference between Tritrp3 and Tritrp7 appears to be in the clustering of the aromatic rings. The tryptophan side chains of Tritrp7 are clustered in a similar fashion as those in the turn-turn structures, with the indole rings of Trp-6 and Trp-7 perpendicular to each other and with the indole ring of Trp-8 stacked on top of the ring of Trp-7. The phenylalanine and tryptophan side chains of Tritrp3 are less compact than those in the turn-turn structures and Tritrp7. The orientations of the aromatic side chains of Tritrp3 more closely resemble those we have previously observed for the helical NMR structure of the 19-residue tryptophan-rich region of gp41 DPC micelles (44), which forms a collar of aromatic resides on either side of the helix backbone. It is noteworthy that the chemical shift of the amide proton of Trp-7 is not significantly upfield shifted in Tritrp3 ($\delta = 7.31$), but in Tritrp7 the Trp-7 amide chemical shift ($\delta = 6.66$) is in between that found in Tritrp3 and the turn-turn peptides (average $\delta = 5.97$), likely due to possible hydrogen bonding of the amide of Trp-7 in the helical structures and the reduced packing of the indole side chains.

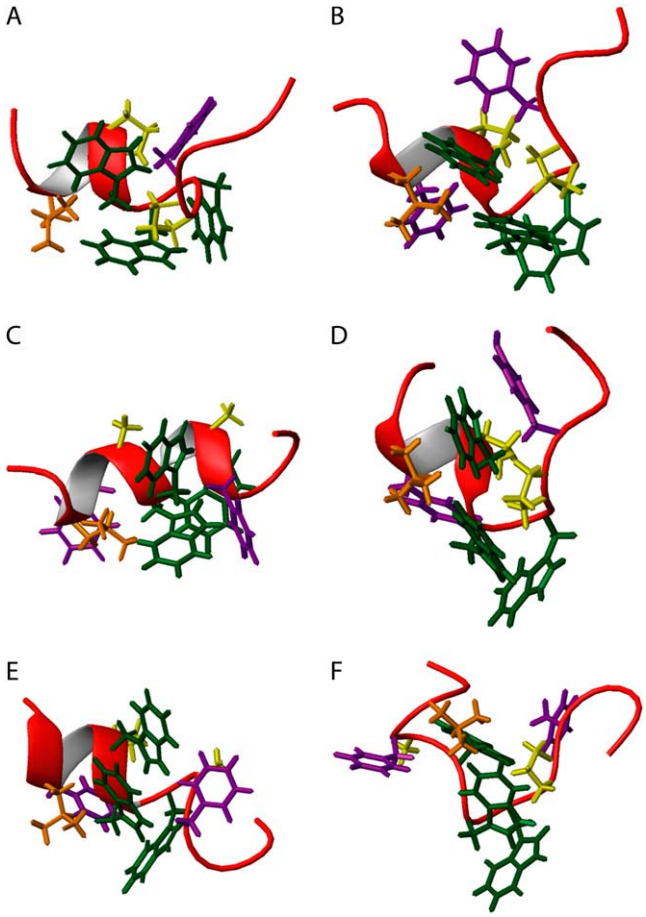

FIGURE 6 Representative ribbon structures of the Tritrp analogs in DPC micelles. (*A*) Tritrp1, (*B*) Tritrp2, (*C*) Tritrp3, (*D*) Tritrp5, (*E*) Tritrp7, and (*F*) Tritrp8. The side chains of the Trp residues are displayed in dark green, the Phe or Tyr residues in dark violet, the Pro or Ala residues in yellow, and the Leu residue in dark orange. The side chains of the basic residues, as well as the terminal valine side chain have been removed for clarity. All structures are in approximately the same orientation, with the C-terminus on the left and the N-terminus on the right.

DISCUSSION

Most studies concerning a structure-function analysis of antimicrobial peptides reported to date compare the structure of a native peptide with an analog that has improved function ((7,45) for examples). In this work our objective was to make comparisons across a larger group of closely related peptides with different activities. Three classes of structures were observed for this group of eight tritrpticin analogs when bound to DPC micelles. For those analogs that do not have any alterations in the central Trp residues or the first Pro residue, an amphipathic turn-turn structure is formed, similar to the original NMR solution structure we reported for tritrpticin in SDS micelles (10). The structures appear to be determined more by intramolecular side chain–side chain interactions and interactions with the DPC detergent (hydrophobic and electrostatic), than by intramolecular hydrogen

bonds. However, some weak hydrogen bonds are likely present, forming the C-terminal helical turn and stabilizing the turn around residues 5–8. This still leaves a large proportion of nonbonded hydrogen bonded donors and acceptors, for which an energetic penalty must be paid after insertion into either micelles or phospholipid bilayers. This penalty is likely compensated by the abundance of aromatic and hydrophobic residues in the central portion of the peptide (43).

The second structural class includes the peptides that adopt more linear helical structures due to the replacement of the first Pro residue in the sequence. The replacement of Pro5 in both Tritrp3 and 7 allows the C-terminal helix to extend the full length of the peptide. The helical class of structures retains the amphipathicity observed for the turn-turn structures, although the helical nature causes the cationic residues to be extended, with the short aliphatic alanine side chains filling in the gap. The formation of a helix for the Pro to Ala analog of tritrpticin in micelles has previously been suggested on the basis of CD spectroscopy data (12). As the majority of the aromatic residues and the hydrophobic leucine side chain are on the opposing face from the alanine residues, it is more likely that the alanines would be positioned away from the hydrophobic core of a micelle or phospholipid bilayer. The NMR structure of a Pro→Ala derivative of indolicidin, also indicates an α-helical amphipathic structure (7).

The third structural class observed in these studies includes Tritrp4 and 6, in which the central Trp residues were replaced by either Tyr or Phe residues. While all of the peptides in this study adopt multiple conformations in aqueous solution on the NMR timescale (with the exception of Tritrp3, which has no Pro residues), Tritrp4 and 6 retain their multiple conformations even in the presence of detergent micelles. This is probably related to their lower affinity for the micelles compared to the Trp-containing peptides. This is consistent with thermodynamic predictions for whole amino acid residues made by Wimley and White (17) of less favorable partitioning between these two Trp-substituted peptides and the membrane interface.

In this study, there are many hints as to possible mechanisms why some peptides may retain antimicrobial activity yet not induce hemolysis, but in most cases there are also exceptions to any proposed mechanisms. Therefore the attribution of hemolysis to Trp as has been suggested (12) may be an oversimplification of the relationship between tryptophan and the hemolytic mechanism. While there is a reasonable correlation between antimicrobial activity, membrane bilayer perturbations, and the structures of the many peptides in this study, the data for Tritrp6, the analog in which the Trp are replaced with Phe, clearly does not fit with the model of the phospholipid bilayer being the primary target for its antimicrobial activity. Tritrp6 is one of the most active peptides used in this study (Table 2) with no detectable hemolytic activity, yet it appears to have a very low membrane perturbing activity as demonstrated in both the calcein leakage assays (Fig. 1) and the lipid flip-flop assay (Fig. 2). Buforin 2, a 21-residue cationic antimicrobial peptide that does not kill bacteria by membrane disruption (46), has a similar pattern of antimicrobial activity and low membrane disruption characteristics as Tritrp6 (47). Although buforin 2 causes little membrane perturbation, it does translocate across phospholipid bilayers (38), and it has an alternative intracellular mode of action (47). Such mechanisms have also been inferred for short Trp- and Arg-rich antimicrobial hexapeptides and heptapeptides (19–21). Additionally, Arg/Pro-rich antimicrobial peptides, such as PR-39, will also translocate bacterial membranes without leading to cell lysis, but instead target intracellular macromolecular processes (1,48,49). Tritrp6 likely acts in a similar manner as these peptides.

There is a strong relationship between the hemolytic activities of these peptides (Table 2) and the degree to which they cause leakage from ePC:cholesterol LUVs (Fig. 1 *E*). The latter membrane mimetic system seems to be a good indicator of lysis in red blood cells. Most of the peptides that had low hemolytic activity also had low flip-flop activity. The weaker hemolytic behavior of Tritrp4 and 6 may be related to their weaker binding to phospholipid bilayers. The relatively low hemolytic character of Tritrp2 compared to the parent compound Tritrp1 must be explained by examining differences between the interactions of the cationic side chains of Arg and Lys with the different phospholipids found in the membranes of bacterial and mammalian cells. For example, in contrast to the amino group, the guanidino group causes the positive charge to be spread out over three nitrogen groups and it also has extensive potential for making several hydrogen bonds. Therefore, while at long range both residues are cationic and contribute to electrostatic effects, at short range these differences cause their side chains to interact with PC and PE headgroups in a different manner. Furthermore, cation-π interactions are possible between the guanidino groups of the Arg side chains and the indole π-electrons of the Trp side chains (1). These stable interactions are thought to shield the positive charge of Arg, thereby making it more favorable for the peptide to cross the hydrophobic core of bacterial membranes. This difference could be observed in the different kinetics measured in the calcein leakage experiments in Fig. 1, where only Tritrp2 showed slow kinetics. It is interesting that in PE and PE/PG lipid systems, there is often very little difference observed in the effects of different charged residues in transmembrane peptides on the phase behavior of phospholipids (50); yet in PC containing lipid systems, differences have been observed in the phase transition behavior induced by Arg and Lys residues (51). Such effects may explain why Tritrp1 causes significant hemolysis in red blood cells and substantial leakage from ePC:cholesterol LUVs whereas Tritrp2 does not.

The structural similarities between Tritrp3 and Tritrp7, with Pro-5 substituted, would suggest that these two helical peptides could have similar interactions with phospholipid bilayers. However, significant differences were observed in

their hemolytic activities (Table 2) and membrane interactions (Figs. 1 and 2). Different Pro→Ala and Pro→Gly analogs of indolicidin and other antimicrobial peptides have been observed to not significantly alter their antimicrobial activity and yet make the peptides more hemolytic (8,52). The aromatic residues of Tritrp3 form a collar around the helical axis of the peptide, in a similar manner to the Trp-rich membrane-proximal peptide of HIV gp41 (44). This gp41 peptide is extremely hemolytic and can cause significant leakage from phospholipid vesicles even at low peptide/lipid ratios ((53); unpublished data). It is possible that the specific positioning of the aromatic residues in a membrane interface by a helical structure is key to membrane disruption of red blood cells.

If all short (<25 residues) cationic antimicrobial peptides are compared to each other in an attempt to correlate membrane perturbation effects with antimicrobial activity there does not appear to be a definitive link (6,7,21,54). However, as this study has demonstrated, highly related peptides can often have very different biophysical properties, which cannot be directly correlated to their biological activities. Therefore, a single unifying theory for large groups of peptides, especially for those that have large differences in both sequence and structure, may not be applicable. This study and others that have not observed a direct correlation between membrane perturbation properties and MIC values (6,55) definitely lends support to the notion that there are additional targets for bactericidal activity. These targets could include the outer components of the bacteria, composed mainly of lipopolysaccharide on Gram negative bacteria and lipoteichoic acid on Gram positive bacteria (55), or intracellular components (56). In such cases, the antimicrobial activity would be determined by the sum of all of the effects of the peptide on the outer membrane and the cytoplasmic membrane and by binding to intracellular targets. By making changes in the peptide sequence, the ratio between these distinct bactericidal activities could alter, yet the overall antimicrobial effect could still be the same. Be that as it may, we can not exclude at this stage that the assays that are used may be oversimplified: i.e., LUVs that only contain one or two lipids differ significantly from the complex membrane environment of bacteria. Therefore the complicated relationships between amino acid composition, sequence, three dimensional structure, membrane interactions, antimicrobial activity, and hemolytic activity may not be easily explained by simple rules where one specific amino acid or one unique secondary structure is always responsible for a specific characteristic.

The atomic coordinates for the tritrpticin analogs (codes 2I1D (Tritrp1); 2I1E (Tritrp2); 2I1F (Tritrp3); 2I1G (Tritrp5); 2I1H (Tritrp7); and 2I1I (Tritrp8)) have been deposited in the Protein Data Bank, Research Collaboratory for Structural Bioinformatics, Rutgers State University, New Brunswick, NJ.

The authors thank Dr. Howard Hunter for many insightful discussions and Dr. Deane McIntyre for management and upkeep of the NMR facilities.

This work was supported by an operating grant from the Canadian Institute for Health Research (CIHR) to H.J.V. D.J.S. and L.T.N. were supported by Alberta Heritage Foundation for Medical Research (AHFMR) studentship awards, whereas H.J.V. holds a Scientist Award from the AHFMR. Maintenance of the NMR facility is supported by the CIHR. The BioNMR Centre was recently upgraded with funds provided by the Canada Foundation for Innovation, the Alberta Science and Research Authority, and the Alberta Heritage Foundation for Medical Research.

REFERENCES

1. Chan, D. I., E. J. Prenner, and H. J. Vogel. 2006. Tryptophan- and arginine-rich antimicrobial peptides: structures and mechanism of action. *Biochim. Biophys. Acta*. In press.
2. Selsted, M. E., M. J. Novotny, W. L. Morris, Y. Q. Tang, W. Smith, and J. S. Cullor. 1992. Indolicidin, a novel bactericidal tridecapeptide amide from neutrophils. *J. Biol. Chem.* 267:4292–4295.
3. Falla, T. J., and R. E. Hancock. 1997. Improved activity of a synthetic indolicidin analog. *Antimicrob. Agents Chemother.* 41:771–775.
4. Subbalakshmi, C., V. Krishnakumari, R. Nagaraj, and N. Sitaram. 1996. Requirements for antibacterial and hemolytic activities in the bovine neutrophil derived 13-residue peptide indolicidin. *FEBS Lett.* 395:48–52.
5. Subbalakshmi, C., E. Bikshapathy, N. Sitaram, and R. Nagaraj. 2000. Antibacterial and haemolytic activities of single tryptophan analogs of indolicidin. *Biochem. Biophys. Res. Commun.* 274:714–716.
6. Friedrich, C. L., D. Moyles, T. J. Beveridge, and R. E. Hancock. 2000. Antibacterial action of structurally diverse cationic peptides on gram-positive bacteria. *Antimicrob. Agents Chemother.* 44:2086–2092.
7. Friedrich, C. L., D. Moyles, T. J. Beveridge, and R. E. Hancock. 2001. Structure and mechanism of action of an indolicidin peptide derivative with improved activity against Gram-positive bacteria. *J. Biol. Chem.* 276:24015–24022.
8. Staubitz, P., A. Peschel, W. F. Nieuwenhuizen, M. Otto, F. Gotz, G. Jung, and R. W. Jack. 2001. Structure-function relationships in the tryptophan-rich, antimicrobial peptide indolicidin. *J. Pept. Sci.* 7: 552–564.
9. Lawyer, C., S. Pai, M. Watabe, P. Borgia, T. Mashimo, L. Eagleton, and K. Watabe. 1996. Antimicrobial activity of a 13 amino acid tryptophan-rich peptide derived from a putative porcine precursor protein of a novel family of antibacterial peptides. *FEBS Lett.* 390: 95–98.
10. Schibli, D. J., P. M. Hwang, and H. J. Vogel. 1999. Structure of the antimicrobial peptide tritrpticin bound to micelles: a distinct membrane-bound peptide fold. *Biochemistry.* 38:16749–16755.
11. Nagpal, S., V. Gupta, K. J. Kaur, and D. M. Salunke. 1999. Structure-function analysis of tritrypticin, an antibacterial peptide of innate immune origin. *J. Biol. Chem.* 274:23296–23304.
12. Yang, S. T., S. Y. Shin, Y. C. Kim, Y. Kim, K. S. Hahm, and J. I. Kim. 2002. Conformation-dependent antibiotic activity of tritrpticin, a cathelicidin-derived antimicrobial peptide. *Biochem. Biophys. Res. Commun.* 296:1044–1050.
13. Yang, S. T., S. Y. Shin, C. W. Lee, Y. C. Kim, K. S. Hahm, and J. I. Kim. 2003. Selective cytotoxicity following Arg-to-Lys substitution in tritrpticin adopting a unique amphipathic turn structure. *FEBS Lett.* 540: 229–233.
14. Pungercar, J., B. Strukelj, G. Kopitar, M. Renko, B. Lenarcic, F. Gubensek, and V. Turk. 1993. Molecular cloning of a putative homolog of proline/arginine-rich antibacterial peptides from porcine bone marrow. *FEBS Lett.* 336:284–288.
15. Strom, M. B., B. E. Haug, O. Rekdal, M. L. Skar, W. Stensen, and J. S. Svendsen. 2002. Important structural features of 15-residue lactoferricin derivatives and methods for improvement of antimicrobial activity. *Biochem. Cell Biol.* 80:65–74.
16. Kyte, J., and R. F. Doolittle. 1982. A simple method for displaying the hydropathic character of a protein. *J. Mol. Biol.* 157:105–132.

17. Wimley, W. C., and S. H. White. 1996. Experimentally determined hydrophobicity scale for proteins at membrane interfaces. *Nat. Struct. Biol.* 3:842–848.

18. Rozek, A., C. L. Friedrich, and R. E. Hancock. 2000. Structure of the bovine antimicrobial peptide indolicidin bound to dodecylphosphocholine and sodium dodecyl sulfate micelles. *Biochemistry.* 39:15765–15774.

19. Herbig, M. E., K. Weller, U. Krauss, A. G. Beck-Sickinger, H. P. Merkle, and O. Zerbe. 2005. Membrane surface-accosiated helices promote lipid interactions and cellular uptake of human calcitonin-derived cell penetrating peptides. *Biophys. J.* 89:4056–4066.

20. Hunter, H. N., W. Jing, D. J. Schibli, T. Trinh, I. Y. Park, S. C. Kim, and H. J. Vogel. 2005. The interactions of antimicrobial peptides derived from lysozyme with model membrane systems. *Biochim. Biophys. Acta.* 1668:175–189.

21. Nguyen, L. T., D. J. Schibli, and H. J. Vogel. 2005. Structural studies and model membrane interactions of two peptides derived from bovine lactoferricin. *J. Pept. Sci.* 11:379–389.

22. Rezansoff, A. J., H. N. Hunter, W. Jing, I. Y. Park, S. C. Kim, and H. J. Vogel. 2005. Interactions of the antimicrobial peptide Ac-FRWWHR-NH(2) with model membrane systems and bacterial cells. *J. Pept. Res.* 65:491–501.

23. Schibli, D. J., R. F. Epand, H. J. Vogel, and R. M. Epand. 2002. Tryptophan-rich antimicrobial peptides: comparative properties and membrane interactions. *Biochem. Cell Biol.* 80:667–677.

24. Schibli, D. J., P. M. Hwang, and H. J. Vogel. 1999. The structure of the antimicrobial active center of lactoferricin B bound to sodium dodecyl sulfate micelles. *FEBS Lett.* 446:213–217.

25. Strom, M. B., O. Rekdal, and J. S. Svendsen. 2002. Antimicrobial activity of short arginine- and tryptophan-rich peptides. *J. Pept. Sci.* 8:36–43.

26. Matsuzaki, K., O. Murase, N. Fujii, and K. Miyajima. 1996. An antimicrobial peptide, magainin 2, induced rapid flip-flop of phospholipids coupled with pore formation and peptide translocation. *Biochemistry.* 35:11361–11368.

27. Olson, F., C. A. Hunt, F. C. Szoka, W. J. Vail, and D. Papahadjopoulos. 1979. Preparation of liposomes of defined size distribution by extrusion through polycarbonate membranes. *Biochim. Biophys. Acta.* 557:9–23.

28. Mayer, L. D., M. J. Hope, and P. R. Cullis. 1986. Vesicles of variable sizes produced by a rapid extrusion procedure. *Biochim. Biophys. Acta.* 858:161–168.

29. Ames, B. N. 1966. Assay of inorganic phosphate, total phosphate and phosphatases. *Meth. Enzym.* 8:115–118.

30. Callihan, D., J. West, S. Kumar, B. I. Schweitzer, and T. M. Logan. 1996. Simple, distortion-free homonuclear spectra of peptides and nucleic acids in water using excitation sculpting. *J. Mag. Res. B.* 112:82–85.

31. Sklenar, V., M. Piotto, R. Leppik, and V. Saudek. 1993. Gradient-tailored water suppression for ^{1}H-^{15}N HSQC experiments optimized to retain full sensitivity. *J. Magn. Reson. A.* 102:241–245.

32. Delaglio, F., S. Grzesiek, G. Vuister, G. Zhu, J. Pfeifer, and A. Bax. 1995. NMRPipe: a multidimensional spectral processing system based on UNIX pipes. *J. Biomol. NMR.* 6:277–293.

33. Johnson, B. A., and R. A. Blevins. 1994. NMR view: a computer program for the visualization and analysis of NMR data. *J. Biomol. NMR.* 4:603–614.

34. Wüthrich, K. 1986. NMR of Proteins and Nucleic Acids. John Wiley and Sons, New York.

35. Nilges, M. 1995. Calculation of protein structures with ambiguous distance restraints. Automated assignment of ambiguous NOE cross-peaks and disulphide connectivities. *J. Mol. Biol.* 245:645–660.

36. Nilges, M. 1997. Ambiguous distance data in the calculation of NMR structures. *Fold. Des.* 2:S53–S57.

37. Nilges, M., and S. I. O'Donoghue. 1998. Ambiguous NOEs and automated NOE assignment. *Prog. NMR Spec.* 32:107–139.

38. Linge, J. P., and M. Nilges. 1999. Influence of non-bonded parameters on the quality of NMR structures: a new force field for NMR structure calculation. *J. Biomol. NMR.* 13:51–59.

39. Falla, T. J., D. N. Karunaratne, and R. E. Hancock. 1996. Mode of action of the antimicrobial peptide indolicidin. *J. Biol. Chem.* 271: 19298–19303.

40. Lohner, K. 2001. The role of membrane lipid composition in cell targeting of antimicrobial peptides. *In* Development of Novel Antimicrobial Agents: Emerging Strategies. K. Lohner, editor. Horizon Scientific Press, Wymondham, Norfolk, UK. 149–165.

41. Matsuzaki, K. 1999. Why and how are peptide-lipid interactions utilized for self-defense? Magainins and tachyplesins as archetypes. *Biochim. Biophys. Acta.* 1462:1–10.

42. Epand, R. M., and H. J. Vogel. 1999. Diversity of antimicrobial peptides and their mechanisms of action. *Biochim. Biophys. Acta.* 1462:11–28.

43. Vogel, H. J., D. J. Schibli, W. Jing, E. M. Lohmeier-Vogel, R. F. Epand, and R. M. Epand. 2002. Towards a structure-function analysis of bovine lactoferricin and related tryptophan- and arginine-containing peptides. *Biochem. Cell Biol.* 80:49–63.

44. Schibli, D. J., R. C. Montelaro, and H. J. Vogel. 2001. The membrane-proximal tryptophan-rich region of the HIV glycoprotein, gp41, forms a well-defined helix in dodecylphosphocholine micelles. *Biochemistry.* 40:9570–9578.

45. Rosengren, K. J., U. Goransson, L. Otvos, Jr., and D. J. Craik. 2004. Cyclization of pyrrhocoricin retains structural elements crucial for the antimicrobial activity of the native peptide. *Biopolymers.* 76:446–458.

46. Park, C. B., M. S. Kim, and S. C. Kim. 1996. A novel antimicrobial peptide from Bufo bufo gargarizans. *Biochem. Biophys. Res. Commun.* 218:408–413.

47. Kobayashi, S., K. Takeshime, C. B. Park, S. C. Kim, and K. Matsuzaki. 2000. Interactions of the novel antimicrobial peptide buforin 2 with lipid bilayers: proline as a translocation promoting factor. *Biochemistry.* 39:8648–8654.

48. Gennaro, R., M. Zanetti, M. Benincasa, E. Podda, and M. Miani. 2002. Pro-rich antimicrobial peptides from animals: structure, biological functions and mechanism of action. *Curr. Pharm. Des.* 8:763–778.

49. Gaczynska, M., P. A. Osmulski, Y. Gao, M. J. Post, and M. Simons. 2003. Proline- and arginine-rich peptides constitute a novel class of allosteric inhibitors of proteasome activity. *Biochemistry.* 42:8663–8670.

50. Strandberg, E., S. Morein, D. T. Rijkers, R. M. Liskamp, P. C. Van Der Wel, and J. A. Killian. 2002. Lipid dependence of membrane anchoring properties and snorkeling behavior of aromatic and charged residues in transmembrane peptides. *Biochemistry.* 41:7190–7198.

51. de Planque, M. R., J. W. Boots, D. T. Rijkers, R. M. Liskamp, D. V. Greathouse, and J. A. Killian. 2002. The effects of hydrophobic mismatch between phosphatidylcholine bilayers and transmembrane alpha-helical peptides depend on the nature of interfacially exposed aromatic and charged residues. *Biochemistry.* 41:8396–8404.

52. Thennarasu, S., and R. Nagaraj. 1996. Specific antimicrobial and hemolytic activities of 18-residue peptides derived from the amino terminal region of the toxin pardaxin. *Protein Eng.* 9:1219–1224.

53. Suarez, T., W. R. Gallaher, A. Agirre, F. M. Goni, and J. L. Nieva. 2000. Membrane interface-interacting sequences within the ectodomain of the human immunodeficiency virus type 1 envelope glycoprotein: putative role during viral fusion. *J. Virol.* 74:8038–8047.

54. Wu, M., E. Maier, R. Benz, and R. E. Hancock. 1999. Mechanism of interaction of different classes of cationic antimicrobial peptides with planar bilayers and with the cytoplasmic membrane of Escherichia coli. *Biochemistry.* 38:7235–7242.

55. Farnaud, S., C. Spiller, L. C. Moriarty, A. Patel, V. Gant, E. W. Odell, and R. W. Evans. 2004. Interactions of lactoferricin-derived peptides with LPS and antimicrobial activity. *FEMS Microbiol. Lett.* 233:193–199.

56. Otvos, L. Jr. 2005. Antimicrobial peptides and proteins with multiple cellular targets. *J. Pept. Sci.* 11:697–706.